

Interaction effect in a \mathcal{PT} -symmetric Bose-Einstein Condensate

Xiaoling Cui^{1, 2, *}

¹*Beijing National Laboratory for Condensed Matter Physics,
Institute of Physics, Chinese Academy of Sciences, Beijing 100190, China*
²*Songshan Lake Materials Laboratory, Dongguan, Guangdong 523808, China*

(Dated: April 1, 2025)

We investigate the ground state and excitation properties of a weakly interacting Bose-Einstein Condensate(BEC) under a parity-time(\mathcal{PT}) symmetric potential with balanced gain and loss. It is shown that the \mathcal{PT} -symmetry, as preserved by the macroscopic condensate, can be spontaneously broken by its Bogoliubov quasi-particles. The associated \mathcal{PT} -breaking transitions in the Bogoliubov spectrum can be conveniently tuned by the interaction anisotropy of BEC and the strength of \mathcal{PT} potential. In the \mathcal{PT} -unbroken regime, the real Bogoliubov modes are generally gapped, in contrast to the Hermitian case with gapless phonon mode. Moreover, it is found that the presence of \mathcal{PT} potential can enhance the mean-field collapse and thereby intrigue the droplet formation after incorporating the repulsive force from quantum fluctuations. These remarkable interplay effects of \mathcal{PT} -symmetry and interaction can be directly probed in cold atoms experiments, which shed light on intriguing collective phenomena in other non-Hermitian systems with \mathcal{PT} -symmetry.

Introduction. The parity-time(\mathcal{PT}) symmetry governs a fascinating class of non-Hermitian Hamiltonians whose energy spectra are purely real and bounded below[1], analogous to the Hermitian ones. Nevertheless, very different from the Hermitian counterpart, the eigenstates of non-Hermitian system are generally non-orthogonal and can even coalesce at the exceptional point(EP), where the \mathcal{PT} -symmetry breaking transition occurs and the eigen-energies after the transition become complex[2]. The \mathcal{PT} -symmetric Hamiltonian and the associated \mathcal{PT} -breaking transitions have been successfully explored earlier in various photonic, electronic and acoustic systems (see reviews [3, 4]), and very recently also in the quantum walk interferometer[5], superconducting circuit[6], nitrogen-vacancy center[7], trapped ions[8, 9] and ultracold gases[10–12].

The interplay of \mathcal{PT} -symmetry and interaction has become a rapidly developing frontier in the study of non-Hermitian physics[13–25]. For instance, such interplay effect has been utilized to engineer high-order EPs with ultra-sensitivity[18], enhance fermion superfluidity[20, 25] and induce intriguing quantum critical phenomena associated with EPs[16, 21, 22]. Here, we aim at a new direction in this frontier area, i.e., the interplay of \mathcal{PT} -symmetry and interaction in affecting the fundamental property of Bose-Einstein Condensates(BECs). Specifically, we consider the two-species (\uparrow, \downarrow) bosons under a \mathcal{PT} -symmetric potential with balanced gain and loss

$$H_{\text{PT}} = \Omega(\sigma_x + i\gamma\sigma_z), \quad (1)$$

where $\sigma_\alpha (\alpha = x, y, z)$ is the Pauli matrix. Obviously $[H_{\text{PT}}, \mathcal{PT}] = 0$, with \mathcal{P} flipping the spin ($\uparrow \leftrightarrow \downarrow$) and \mathcal{T} changing i to $-i$. The single-particle physics of H_{PT} as been widely explored in literature[3–12], and the \mathcal{PT} -breaking transition of the eigen-states occurs at $\gamma = 1$.

In this work we will develop a systematic theory for the ground state and excitation properties of a weakly

interacting BEC under H_{PT} . We focus on the regime $\gamma < 1$, such that the \mathcal{PT} -symmetry is preserved by the macroscopic condensate. Interestingly, it is found that the \mathcal{PT} -symmetry can be spontaneously broken by the Bogoliubov quasi-particles, and the location of \mathcal{PT} -breaking transition in the Bogoliubov spectrum sensitively depends on the strength of H_{PT} and the interaction anisotropy of BEC. In the \mathcal{PT} -unbroken regime, a remarkable feature is that the Bogoliubov modes are generally gapped, contrary to the gapless phonon mode in Hermitian case. This can be attributed to the cooperative effect of interaction anisotropy and non-orthogonality of single-particle eigenstates, and thus is unique for non-Hermitian system. Moreover, the presence of H_{PT} can enhance the mean-field collapse of BEC and facilitate the droplet formation in a broader interaction regime than the Hermitian counterpart. Experimental relevance of our results and the implication to a general \mathcal{PT} -symmetric system will also be discussed.

Model. We consider the following Hamiltonian for two-species bosons ($\hbar = 1$ throughout the paper)

$$H = \int d\mathbf{r} \sum_{\alpha\beta} \left\{ \Psi_\alpha^\dagger(\mathbf{r}) \left[-\frac{\nabla^2}{2m_\alpha} \delta_{\alpha\beta} + \Omega(\sigma_x^{\alpha\beta} + i\gamma\sigma_z^{\alpha\beta}) \right] \Psi_\beta(\mathbf{r}) \right. \\ \left. + \frac{g_{\alpha\beta}}{2} \Psi_\alpha^\dagger(\mathbf{r}) \Psi_\beta^\dagger(\mathbf{r}) \Psi_\beta(\mathbf{r}) \Psi_\alpha(\mathbf{r}) \right\}. \quad (2)$$

Here $\alpha, \beta = \{\uparrow, \downarrow\}$, and $\{\Psi_\alpha^\dagger, \Psi_\alpha\}$ are the field operators of spin- α bosons. In order to ensure the \mathcal{PT} -symmetry of (2), we take the equal mass $m_\uparrow = m_\downarrow \equiv m$ and equal intra-species coupling $g_{\uparrow\uparrow} = g_{\downarrow\downarrow} \equiv g$. In this case, the property of a homogeneous BEC is determined by three dimensionless parameters: γ , $\eta \equiv g_{\uparrow\downarrow}/g$ and $\tilde{\Omega} \equiv \Omega/(gn)$, with n the total density of the BEC.

The non-interacting part of (2) can be diagonalized as

$$H_0 = \sum_\nu \epsilon_{\nu\mathbf{k}} \Psi_{\nu\mathbf{k},R}^\dagger \Psi_{\nu\mathbf{k},L} \quad (3)$$

where $\nu = \{+, -\}$ is the index of single-particle eigenstate with eigen-energy $\epsilon_{\nu\mathbf{k}} = \mathbf{k}^2/(2m) + \nu\Omega\sqrt{1-\gamma^2}$; $\Psi_{\nu\mathbf{k},R}^\dagger$ ($\Psi_{\nu\mathbf{k},L}$) is the associated creation (annihilation) operator of the right (left) eigenstate, which satisfies the commutation relation[26]

$$[\Psi_{\nu'\mathbf{k}',L}, \Psi_{\nu\mathbf{k},R}^\dagger] = \delta_{\mathbf{k}\mathbf{k}'}\delta_{\nu\nu'}. \quad (4)$$

This relation is equivalent to the bi-orthogonality of right and left eigen-states, which is crucially important for building up the theory of non-Hermitian BEC as below.

In the mean-field framework, we can write down a general coherent ansatz for the right state of the BEC:

$$|\Psi_0\rangle_R = \mathcal{A} \sum_n \frac{(\sum_\nu \sqrt{N_\nu} e^{i\theta_\nu} \Psi_{\nu\mathbf{k}=0,R}^\dagger)^n}{n!} |0\rangle. \quad (5)$$

Here $|0\rangle$ is the vacuum, N_ν and θ_ν are respectively the mean number and the phase of the condensate at level ν . In the regime $\gamma < 1$, since the single-particle state $\Psi_{\nu\mathbf{k},R/L}^\dagger |0\rangle$ preserves the \mathcal{PT} -symmetry, it is natural to require the condensate (5) equally preserve such symmetry. By choosing a specific gauge that $\mathcal{PT}\Psi_{\nu\mathbf{k},R/L}^\dagger |0\rangle = \nu u^* \Psi_{\nu\mathbf{k},R/L}^\dagger |0\rangle$ [26], this requirement leads to $e^{2i\theta_\nu} = \nu u^*$. Following the same strategy, we can obtain the left state of the BEC, $|\Psi_0\rangle_L$, which shares the same form as (5) except replacing $\Psi_{\nu\mathbf{k}=0,R}^\dagger$ by $\Psi_{\nu\mathbf{k}=0,L}^\dagger$. The specific gauge choice will not influence the physical quantities studied in this work.

Taking advantage of Eq.(4), the final step of the mean-field treatment is to replace the zero-momentum operators $\Psi_{\nu\mathbf{k}=0,R}^\dagger$ and $\Psi_{\nu\mathbf{k}=0,L}^\dagger$ by their mean values under the bi-orthogonal basis ${}_L\langle\Psi_0| \dots |\Psi_0\rangle_R$ [26]:

$$\Psi_{\nu\mathbf{k}=0,R}^\dagger \rightarrow \sqrt{N_\nu} e^{-i\theta_\nu}, \quad \Psi_{\nu\mathbf{k}=0,L}^\dagger \rightarrow \sqrt{N_\nu} e^{i\theta_\nu}. \quad (6)$$

To facilitate later discussions, we rewrite the interaction part of (2) in the following form:

$$U = \sum_{\nu_1\nu_2\nu_3\nu_4} U_{\nu_1\nu_2;\nu_3\nu_4} \sum_{\mathbf{Q}\mathbf{k}\mathbf{k}'} \Psi_{\nu_1\mathbf{Q}-\mathbf{k},R}^\dagger \Psi_{\nu_2\mathbf{k},R}^\dagger \Psi_{\nu_3\mathbf{k}',L} \Psi_{\nu_4\mathbf{Q}-\mathbf{k}',L} \quad (7)$$

Here $U_{\nu_1\nu_2;\nu_3\nu_4}$ is invariant under the permutation of $\nu_1 \leftrightarrow \nu_2$ or $\nu_3 \leftrightarrow \nu_4$, and thus there are totally nine different coupling channels, with five even-parity combinations $\{\nu_1\nu_2; \nu_3\nu_4\} = \{++; ++\}, \{--; --\}, \{++; --\}, \{--; ++\}, \{+-; +-\}$, and four odd-parity ones $\{+-; ++\}, \{+-; --\}, \{++; +-\}, \{--; +-\}$ [26]. Note that the coupling strengths of odd-parity channels are proportional to $i\gamma(1-\eta)$, which is non-zero only for non-Hermitian case($\gamma \neq 0$) and with spin-dependent interaction($\eta \neq 1$). As shown later, their existence can significantly affect the excitation property of the BEC.

Mean-field ground state. It is found that the mean-field energy, $E_{\text{mf}} = {}_L\langle\Psi_0|H|\Psi_0\rangle_R$, replies on the parameter $x \equiv N_-/N$, where $N = N_- + N_+$ is the total number. Explicitly, the energy per particle $\epsilon_{\text{mf}} \equiv E_{\text{mf}}/N$ reads

$$\epsilon_{\text{mf}}(x) = \Omega\sqrt{1-\gamma^2}(1-2x) + \frac{gn}{1-\gamma^2} \left(\gamma^2(\eta-1)(x^2-x) + \frac{1-2\gamma^2+\eta}{4} \right) \quad (8)$$

For simplicity, in this work we will focus on the $\eta < 1$ regime, where the minimum of $\epsilon_{\text{mf}}(x)$ locates at $x = 1$, i.e., the bosons condense at the lower branch with energy

$$\epsilon_{\text{mf}} = -\Omega\sqrt{1-\gamma^2} + \frac{gn}{1-\gamma^2} \frac{1-2\gamma^2+\eta}{4}. \quad (9)$$

Accordingly, we can obtain the chemical potential $\mu \equiv \partial E_{\text{mf}}/\partial N$ and further the compressibility $\chi \equiv \partial n/\partial \mu$ as

$$\chi = \frac{2}{g} \frac{1-\gamma^2}{1-2\gamma^2+\eta}. \quad (10)$$

The mean-field stability against density fluctuations would require $\chi > 0$ and thus $\eta > 2\gamma^2 - 1$, which condition is more stringent than the Hermitian case ($\eta > -1$). In other words, a non-Hermitian BEC (with finite γ) can undergo mean-field collapse more easily than its Hermitian counterpart ($\gamma = 0$). This will be responsible for the γ -induced droplet formation as discussed later.

Bogoliubov analysis. Given the \mathcal{PT} -symmetric BEC at $\mathbf{k} = 0$ and $\nu = -$, we now study its elementary excitations. Following the standard Bogoliubov approach, we assume $\Psi_{\nu\mathbf{k},R}^\dagger$ and $\Psi_{\nu\mathbf{k},L}$ (except for $\nu = -, \mathbf{k} = 0$) are all small fluctuation operators and only keep in the Hamiltonian all the bi-linear terms of these operators, which gives $H = N\epsilon_{\text{mf}} + H_{\text{BG}}$ with

$$H_{\text{BG}} = \sum_{\mathbf{k}} \sum_{\nu} \left((\epsilon_{\nu\mathbf{k}} - \mu + gnu_\nu) \Psi_{\nu\mathbf{k},R}^\dagger \Psi_{\nu\mathbf{k},L} + gnu'_\nu (e^{2i\theta_-} \Psi_{\nu\mathbf{k},R}^\dagger \Psi_{\nu;-\mathbf{k},R}^\dagger + e^{-2i\theta_-} \Psi_{\nu\mathbf{k},L} \Psi_{\nu;-\mathbf{k},L}) \right) \\ + gnu'' \sum_{\mathbf{k}} \left(e^{2i\theta_-} \Psi_{+;\mathbf{k},R}^\dagger \Psi_{-;-\mathbf{k},R}^\dagger + e^{-2i\theta_-} \Psi_{+;\mathbf{k},L} \Psi_{-;-\mathbf{k},L} + 2\Psi_{+;\mathbf{k},R}^\dagger \Psi_{-;\mathbf{k},L} + 2\Psi_{-;\mathbf{k},R}^\dagger \Psi_{+;\mathbf{k},L} \right). \quad (11)$$

with coupling strengths

$$u_- = 4u'_- = \frac{1-2\gamma^2+\eta}{1-\gamma^2}; \quad u_+ = \frac{1-\eta\gamma^2}{1-\gamma^2}; \\ u'_+ = \frac{1-\eta}{4(1-\gamma^2)}; \quad u'' = -\frac{i\gamma(1-\eta)}{2(1-\gamma^2)}. \quad (12)$$

Here H_{BG} naturally inherits \mathcal{PT} -symmetry from the full

Hamiltonian (2), since we have taken the condensate (5) as \mathcal{PT} -symmetric. The first line in H_{BG} is reduced from even-parity channels, and the second line from odd-parity ones. Obviously, the effect of odd-parity channels is to couple fluctuations in different branches, and their physical origin can be attributed to the interplay of non-orthogonal eigen-states in non-Hermitian systems and spin-dependent interaction. Therefore, a finite odd-parity coupling ($u'' \neq 0$) requires both non-Hermiticity ($\gamma \neq 0$) and interaction anisotropy ($\eta \neq 1$).

By employing the equations of motion for $\{\Psi_{\nu\mathbf{k},R}^\dagger, \Psi_{\nu\mathbf{k},L}\}$, we can diagonalize H_{BG} as[26]

$$H_{\text{BG}} = \sum'_{\mathbf{k}} \sum_{i=1}^4 E_{i\mathbf{k}} \alpha_{i\mathbf{k},R}^\dagger \alpha_{i\mathbf{k},L} + \text{const}, \quad (13)$$

where $\{\alpha_{i\mathbf{k},R}^\dagger, \alpha_{i\mathbf{k},L}\}$ are the operators for four eigenmodes which obey similar commutation relation as (4); $E_{i\mathbf{k}}$ are the eigen-energies that can be divided to two pairs, say, $E_{1\mathbf{k}} = E_{2\mathbf{k}}$ and $E_{3\mathbf{k}} = E_{4\mathbf{k}}$. Hereafter we only consider the property of $E_{1\mathbf{k}}$ and $E_{3\mathbf{k}}$. The constant term in (13) contributes to the Lee-Huang-Yang(LHY) energy:

$$E_{\text{LHY}} = \frac{1}{2} \sum_{\mathbf{k}} \left\{ E_{1\mathbf{k}} + E_{3\mathbf{k}} - \sum_{\nu} (\epsilon_{\nu\mathbf{k}} - \mu + g n u_{\nu}) + \frac{1 - 2\gamma^2 + \eta^2}{2(1 - \gamma^2)} \frac{m(gn)^2}{\mathbf{k}^2} \right\}. \quad (14)$$

Note that in obtaining (14) we have incorporated the regularization of g and $g_{\uparrow\downarrow}$ from mean-field energy (9).

Excitation spectrum. To highlight the effect of non-Hermiticity to Bogoliubov excitations, we first go through the Hermitian case ($\gamma = 0$). In this case, all odd-parity terms in (11) are absent ($u'' = 0$) and the fluctuations in + and - branches are well decoupled. This leads to a gapless spectrum $E_{1\mathbf{k}} = \sqrt{(\mathbf{k}^2/2m)^2 + 2\mu_- \mathbf{k}^2/(2m)}$ and a gapped one $E_{3\mathbf{k}} = \sqrt{(\mathbf{k}^2/2m + 2\tilde{\Omega})^2 + 2\mu_+ (\mathbf{k}^2/2m + 2\tilde{\Omega})}$, with $\mu_{\pm} = gn(1 \mp \eta)/2$. Clearly, in the mean-field collapse regime with $\eta < -1$, the lower spectrum $E_{1\mathbf{k}}$ becomes purely imaginary near $\mathbf{k} \sim 0$, signifying the dynamical instability. In addition, we note that under certain condition the two spectra become degenerate, i.e., $E_{1,\mathbf{k}_0} = E_{3,\mathbf{k}_0}$ at:

$$|\mathbf{k}_0| = \sqrt{2m\Omega((\eta - 2\tilde{\Omega})^{-1} - 1)}, \quad \text{if } 0 < \eta - 2\tilde{\Omega} < 1. \quad (15)$$

The according plot is given in Fig.2 (a). This feature will lead to interesting excitation property when turn on γ .

In the presence of non-Hermiticity($\gamma \neq 0$), the fluctuations in different branches couple together, and there are two important impacts on Bogoliubov modes:

(I). Spontaneous \mathcal{PT} -symmetry breaking. Although \mathcal{PT} -symmetry is preserved by H , H_{BG} and the condensate $|\Psi_0\rangle_{R,L}$, it can be spontaneously broken by

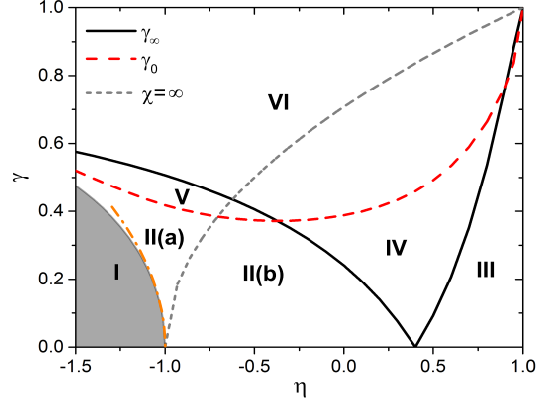


FIG. 1. (Color online). Diagrams in (γ, η) plane that exhibit different excitation properties. Here $\tilde{\Omega} = 0.2$. 'I' marks the region where the excitation spectrum at low- \mathbf{k} is purely imaginary. 'II' is the region where all spectra are real and gapped. The gray dashed line sets the mean-field collapse boundary, which further divides II into II(a) ($\chi < 0$) and II(b) ($\chi > 0$). \mathcal{PT} -breaking transition of Bogoliubov modes occurs in regions III, IV and V, where the spectra become complex either within intermediate $|\mathbf{k}| \equiv k(\text{III})$, or at large $k(\text{IV})$, or low $k(\text{V})$. In VI, the complex spectra occur for all \mathbf{k} . These regions are separated by the curves of γ_0 and γ_∞ , which, respectively, are the values of γ when the spectra becomes complex at $k = 0$ and $k \rightarrow \infty$.

the Bogoliubov quasi-particles, as manifested by the appearance of complex $E_{i\mathbf{k}}$. The \mathcal{PT} -broken region in \mathbf{k} -space sensitively depends on parameters $\tilde{\Omega}$, η and γ . In Fig.1, we have divided (γ, η) plane into different regions (I-VI) according to different \mathcal{PT} -breaking properties in the Bogoliubov spectra for a fixed $\tilde{\Omega} = 0.2$.

Let us start from region III with a small γ and $2\tilde{\Omega} < \eta < 1$ (satisfying the condition in (15)). In this case, a finite γ will lead to the \mathcal{PT} -breaking of excitation spectra near \mathbf{k}_0 . As shown in Fig.2(b1,b2), for $\gamma = 0.15$, $E_{1\mathbf{k}}$ and $E_{3\mathbf{k}}$ are complex and conjugate to each other within a finite window $|\mathbf{k}| \equiv k \in (k_1, k_2)$. Thus, as increasing k from zero, the \mathcal{PT} -symmetry breaks at k_1 and then revives at k_2 . The critical boundaries k_1 , k_2 sensitively depend on γ (Fig.2(c)), and at small γ , they feature a linear shift from k_0 [26]. Continuously increasing γ , k_2 and k_1 respectively flow to ∞ and 0 at γ_∞ and γ_0 . This tells that the spectra at large k become complex if $\gamma > \gamma_\infty$, and the complex spectra extend to $k = 0$ if $\gamma > \gamma_0$.

In Fig.1, γ_0 and γ_∞ are plotted as functions of η , and accordingly regions III-IV are separated. Specifically, the \mathcal{PT} -breaking of Bogoliubov modes occur within a finite k -window in III (with $\gamma < \gamma_0, \gamma_\infty$), at large k in IV ($\gamma_\infty < \gamma < \gamma_0$), at small k in V ($\gamma_0 < \gamma < \gamma_\infty$), and extend the whole k -space in IV($\gamma > \gamma_0, \gamma_\infty$). The typical spectra in regions IV and V are given in Fig.2(d,e). This shows that the \mathcal{PT} -symmetry of Bogoliubov modes can be conveniently tuned by the non-Hermiticity γ and the

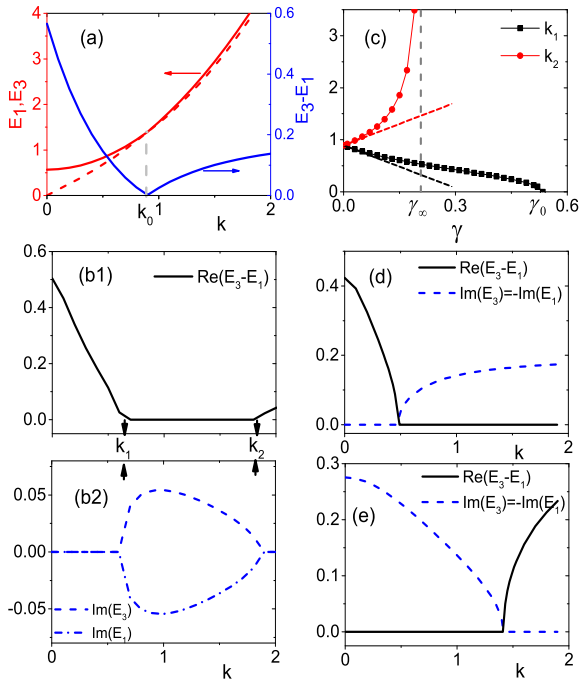


FIG. 2. (Color online). Spontaneous \mathcal{PT} -symmetry breaking in the Bogoliubov spectra. Here $\tilde{\Omega} = 0.2$, and $\eta = 0.6$ for (a-c). (a) Two real spectra for Hermitian case ($\gamma = 0$), which merge at $k \equiv |\mathbf{k}| = k_0$ (see Eq.15). (b1,b2) Real and imaginary parts of the spectra at $\gamma = 0.15$ (staying in region III), which shows \mathcal{PT} -symmetry breaking for $k \in (k_1, k_2)$. (c) \mathcal{PT} -breaking boundaries k_1 and k_2 as functions of γ . Dashed lines show linear fits for small γ (see [26]). k_1 touches zero at γ_0 and k_2 goes to ∞ at γ_∞ . (d) and (e): Excitation spectra for $\eta = 0.4$, $\gamma = 0.3$ (region IV) and for $\eta = -0.8$, $\gamma = 0.45$ (region V), where the \mathcal{PT} -breaking occurs, respectively, at high k and low k . Here the momentum and energy units are, respectively, $\sqrt{2mgn}$ and gn .

interaction anisotropy η .

(II). Gapped excitation. In the \mathcal{PT} -unbroken region, such as II in Fig.1, the real Bogoliubov modes are gapped, instead of gapless as in Hermitian case. For $\gamma \ll 1$, the excitation gap scales linearly with γ :

$$\frac{E_{1,\mathbf{k}=0}}{gn} = \gamma \frac{1-\eta}{2} \sqrt{\frac{1+\eta}{2\tilde{\Omega}}}. \quad (16)$$

The physical origin of such gapped spectrum is, again, related to the odd-parity terms in (11), such as $\Psi_{+;\mathbf{k},R}^\dagger \Psi_{-;\mathbf{k},L}$ which directly excite the lower-branch particle to upper-branch crossing a finite energy gap. As a result, the Bogoliubov excitation is also gapped (see (16)) when these terms are present, i.e., for $\gamma \neq 0$ and $\eta \neq 1$. In Fig.3(a), we extract the energy gap as a function of γ for two typical η , which fit well to (16) in small γ regime.

Interestingly, the gapped excitation appears not only in the mean-field stable regime (region II(a)), but can also extend to the collapse regime (II(b)). This is in distinct

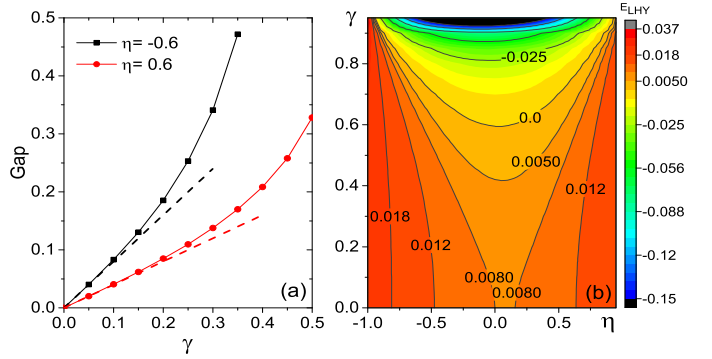


FIG. 3. (Color online). (a) Excitation gap as a function of γ for $\eta = -0.6$ and 0.6 . Dashed lines show the respective function fit according to Eq.16. (b) Contour plot of f -function in the (γ, η) plane. Here $\tilde{\Omega} = 0.2$. The energy unit is gn .

contrast to the Hermitian case where the low- k spectrum is purely imaginary in the mean-field collapse side. It is to say, the mean-field instability in non-Hermitian system does not necessarily lead to imaginary excitations. In fact, for a given $\eta < -1$, the excitation spectra can turn from purely imaginary to purely real as increasing γ across a critical γ_c , at which point the spectrum is gapless $E_{1,\mathbf{k}=0} = 0$. In Fig.1, we mark the $\gamma < \gamma_c$ region ('I') as shaded area. Near $\eta \sim -1$, we have $\gamma_c \propto \sqrt{-(1+\eta)}$ [26], as shown by orange dashed-dot line in Fig.1.

γ-induced droplet. The fact that the non-Hermiticity γ enhances the mean-field collapse (as shown by (10)) renders the formation of a self-bound droplet after incorporating the LHY correction from quantum fluctuations. In general, Eq.(14) gives $\mathcal{E}_{\text{LHY}} \equiv E_{\text{LHY}}/V$ as:

$$\mathcal{E}_{\text{LHY}} = (2m)^{3/2} (gn)^{5/2} f(\gamma, \eta, \tilde{\Omega}) \quad (17)$$

where f is a dimensionless functional. In Fig.3(b), we show the contour plot of f in (γ, η) plane given a fixed $\tilde{\Omega} = 0.2$. We can see that f , or \mathcal{E}_{LHY} , decreases continuously as γ increases and can even turn negative at certain γ . Fortunately, in region II(a), which is the mean-field collapse regime with real and gapped spectra, the LHY force is always repulsive. A droplet with zero pressure can be supported in this region with equilibrium density

$$n_{\text{eq}} = \left(\frac{1-2\gamma^2+\eta}{1-\gamma^2} \right)^2 \frac{1}{36(2m)^3 f^2(\gamma, \eta, \tilde{\Omega})}. \quad (18)$$

A droplet to gas transition would occur if the particle number is below a critical N_c , and following the same strategy in treating the Hermitian droplet [27] we obtain $N_c = 2\sqrt{2}f\tilde{N}_c[6(1-\gamma^2)/|1-2\gamma^2+\eta|]^{5/2}$ [26], with $\tilde{N}_c = 18.65$. We can see that both n_{eq} and N_c can be conveniently tuned by γ and η .

Experimental relevance. A \mathcal{PT} -symmetric two-species BEC can be realized using two hyperfine states of ^{87}Rb

bosons, $|\uparrow\rangle = |F=1, m_F=1\rangle$ and $|\downarrow\rangle = |F=2, m_F=-1\rangle$, which have nearly identical intra-species repulsion with $a_{\uparrow\uparrow} = 95a_B$, $a_{\downarrow\downarrow} = 100a_B$ [28], and the inter-species coupling is highly tunable via Feshbach resonance around $B_0 = 9.1\text{G}$ [29–31]. σ_x term in (1) can be implemented through the two-photon microwave and rf transition[32], and $i\sigma_z$ can be realized using the laser-induced state-selective dissipation up to a constant loss term $i\Omega\gamma$ [10–12]. In this driven-dissipative system, the physics governed by the effective non-Hermitian Hamiltonian can be tested under the post-selection scheme[10, 12], provided that the short-time dynamics is considered with timescale $t \ll 1/(\Omega\gamma)$ and the impact of quantum jump can be neglected. Note that the existing experiments on quantum droplet exactly made use of the atom loss to facilitate the observation of droplet-gas transition[33–37]. We thus expect that the γ -induced droplet can be directly probed in realistic experiments. The property of excitation spectrum can be explored by the Bragg spectroscopy[38–40].

Final remark. The intriguing excitation properties of BEC revealed in this work are closely related to the presence of odd-parity coupling channels, which can be traced back to the fundamental character of non-Hermitian systems, i.e., the non-orthogonality of eigenstates. We thus expect that these properties are not limited to the specific H_{PT} considered here, but can be applicable to a broad class of non-Hermitian systems with \mathcal{PT} -symmetry. Indeed, a recent study has pointed out the spontaneous \mathcal{PT} -breaking of elementary excitations on top of a fermion superfluid[24]. These \mathcal{PT} -breaking phenomena are generally associated with the collective many-body EP and may lead to giant fluctuation effect[21, 22]. It is worth to explore in future the impact of collective EPs in phase and number fluctuations, as well as the property of BEC in other parameter regime beyond the scope of this work.

Acknowledgement. We thank Dajun Wang for helpful discussion on experimental realization of the system. The work is supported by the National Key Research and Development Program of China (2018YFA0307600), the National Natural Science Foundation of China (No.12074419), and the Strategic Priority Research Program of Chinese Academy of Sciences (No. XDB33000000).

* xl cui@iphy.ac.cn

[1] C. M. Bender and S. Boettcher, Phys. Rev. Lett. **80**, 5243 (1998).
[2] N. Moiseyev, *Non-Hermitian Quantum Mechanics* (Cambridge Univ. Press, 2011).
[3] V. V. Konotop, J. Yang, D. A. Zezyulin, Rev. Mod. Phys. **88**, 035002 (2016).
[4] R. El-Ganainy, K. G. Makris, M. Khajavikhan, Z. H. Musslimani, S. Rotter, D. N. Christodoulides, Nat. Phys. **14**, 11 (2018).
[5] L. Xiao, X. Zhan, Z. H. Bian, K. K. Wang, X. Zhang, X. P. Wang, J. Li, K. Mochizuki, D. Kim, N. Kawakami, W. Yi, H. Obuse, B. C. Sanders, and P. Xue, Nat. Phys. **13**, 1117 (2017).
[6] M. Naghiloo, M. Abbasi, Y. N. Joglekar, and K. W. Murch, Nat. Phys. **15**, 1232 (2019).
[7] Y. Wu, W. Liu, J. Geng, X. Song, X. Ye, C.-K. Duan, X. Rong, J. Du, Science **364**, 878 (2019).
[8] L. Ding, K. Shi, Q. Zhang, D. Shen, X. Zhang, and W. Zhang, Phys. Rev. Lett. **126**, 083604 (2021).
[9] W.-C. Wang, Y.-L. Zhou, H.-L. Zhang, J. Zhang, M.-C. Zhang, Y. Xie, C.-W. Wu, T. Chen, B.-Q. Ou, W. Wu, H. Jing, and P.-X. Chen, Phys. Rev. A **103**, L020201 (2021).
[10] J. Li, A. K. Harter, J. Liu, L. de Melo, Y. N. Joglekar, and L. Luo, Nat. Comm. **10**, 855 (2019).
[11] S. Lapp, J. Ang'ong'a, F. Alex An, B. Gadway, New. J. Phys. **21**, 045006 (2019).
[12] Z. Ren, D. Liu, E. Zhao, C. He, K. K. Pak, J. Li, G.-B. Jo, arxiv: 2106.04874.
[13] H. Cartarius and G. Wunner, Phys. Rev. A **86**, 013612 (2012).
[14] D. A. Zezyulin and V. V. Konotop, Phys. Rev. A **94**, 043853 (2016).
[15] V. Tripathi, A. Galda, H. Barman, and V. M. Vinokur, Phys. Rev. B **94**, 041104(R) (2016).
[16] Y. Ashida, S. Furukawa, and M. Ueda, Nat. Commun. **8**, 15791 (2017).
[17] A. Ghatak and T. Das, Phys. Rev. B **97**, 014512 (2018).
[18] L. Pan, S. Chen, and X. Cui, Phys. Rev. A **99**, 011601(R) (2019); ibid, Phys. Rev. A **99**, 063616 (2019).
[19] Z. Zhou and Z. Yu, Phys. Rev. A **99**, 043412 (2019).
[20] L. Zhou and X. Cui, iScience **14**, 257 (2019).
[21] R. Hanai, and P. B. Littlewood, Phys. Rev. Res. **2**, 033018 (2020).
[22] M. Fruchart, R. Hanai, P. B. Littlewood, V. Vitelli, Nature **592**, 363 (2021).
[23] L. Pan, X. Wang, X. Cui, S. Chen, Phys. Rev. A **102**, 023306 (2020).
[24] J.-S. Pan, W. Yi, J. Gong, arxiv:2103.00450.
[25] Y.-M. Li, X.-W. Luo, C. Zhang, arxiv:2107.10391.
[26] See Supplementary Materials for more details on the single-particle and collective properties of BEC under the \mathcal{PT} -symmetric potential.
[27] D.S. Petrov, Phys. Rev. Lett. **115**, 155302 (2015).
[28] Here the relative asymmetry $|a_{\uparrow\uparrow} - a_{\downarrow\downarrow}|/(a_{\uparrow\uparrow} + a_{\downarrow\downarrow}) \sim 2.5\%$, which is expected to take little effect as long as it is much smaller than $\tilde{\Omega}$, γ .
[29] M. Erhard, H. Schmaljohann, J. Kronjäger, K. Bongs, and K. Sengstock, Phys. Rev. A **69**, 032705 (2004);
[30] A. Widera, O. Mandel, M. Greiner, S. Kreim, Theodor W. Hänsch, and I. Bloch, Phys. Rev. Lett. **92**, 160406 (2004).
[31] S. Tojo, Y. Taguchi, Y. Masuyama, T. Hayashi, H. Saito, T. Hirano, Phys. Rev. A **82**, 033609 (2010).
[32] A. M. Kaufman, R. P. Anderson, T. M. Hanna, E. Tiesinga, P. S. Julienne, and D. S. Hall, Phys. Rev. A **80**, 050701(R) (2009).
[33] C.R. Cabrera, L. Tanzi, J. Sanz, B. Naylor, P. Thomas, P. Cheiney, and L. Tarruell, Science **359**, 301 (2018).
[34] P. Cheiney, C. R. Cabrera, J. Sanz, B. Naylor, L. Tanzi, L. Tarruell, Phys. Rev. Lett. **120**, 135301 (2018).
[35] G. Semeghini, G. Ferioli, L. Masi, C. Mazzinghi, L. Wol-

swijk, F. Minardi, M. Modugno, G. Modugno, M. Ingus-
cio, M. Fattori, Phys. Rev. Lett. **120**, 235301 (2018).

[36] C. D'Errico, A. Burchianti, M. Prevedelli, L. Salasnich,
F. Ancilotto, M. Modugno, F. Minardi, and C. Fort,
Phys. Rev. Res. **1**, 033155 (2019).

[37] Z. Guo, F. Jia, L. Li, Y. Ma, J. M. Hutson, X. Cui, D.
Wang, arXiv:2105.01277.

[38] J. Steinhauer, R. Ozeri, N. Katz, and N. Davidson, Phys.
Rev. Lett. **88**, 120407 (2002).

[39] P. T. Ernst, S. Götze, J. S. Krauser, K. Pyka, D.-S.
Lühmann, D. Pfannkuche, and K. Sengstock, Nat. Phys.
6, 56 (2010).

[40] S.-C. Ji, L. Zhang, X.-T. Xu, Z. Wu, Y. Deng, S. Chen,
J.-W. Pan, Phys. Rev. Lett. **114**, 105301 (2015).

[41] L. Zhou, W. Yi and X. Cui, Phys. Rev. A **102**, 043310
(2020).

Supplemental Material

In this Supplemental Material, we provide more details on the microscopic theory of a two-species BEC under a \mathcal{PT} -symmetric potential H_{PT} (Eq.1 in the main text).

I. Right and left eigenstate for single particle in $\gamma < 1$ regime

Since H_{PT} decouples from the kinetic term, here we just focus on the spin part of the single-particle state which is determined solely by H_{PT} . In the regime $\gamma < 1$, the eigen-energies are all real and given by

$$\epsilon_\nu = \nu\Omega\sqrt{1-\gamma^2}, \quad \nu = +, - \quad (19)$$

The right and left eigenvectors, $|\nu\rangle_R$ and $|\nu\rangle_L$, are defined through the Schrödinger equation:

$$H_{\text{PT}}|\nu\rangle_R = \epsilon_\nu|\nu\rangle_R, \quad H_{\text{PT}}^\dagger|\nu\rangle_L = \epsilon_\nu^*|\nu\rangle_L. \quad (20)$$

The eigenvectors read

$$\begin{aligned} |+\rangle_R &= C_{+,R} \begin{pmatrix} u \\ 1 \end{pmatrix}; & |-\rangle_R &= C_{-,R} \begin{pmatrix} 1 \\ -u \end{pmatrix}. \\ |+\rangle_L &= C_{+,L} \begin{pmatrix} 1 \\ u \end{pmatrix}; & |-\rangle_L &= C_{-,L} \begin{pmatrix} u \\ -1 \end{pmatrix}. \end{aligned} \quad (21)$$

Here $u = \sqrt{1-\gamma^2} + i\gamma$, and $C_{\nu,R}, C_{\nu,L}$ are all normalization factors. For the Hermitian case ($\gamma = 0$ and $u = 1$), we can see that the right and left eigenvectors become identical, i.e., $|+\rangle_R \sim |+\rangle_L, |-\rangle_R \sim |-\rangle_L$, and different levels are orthogonal to each other ${}_{R,L}\langle -|+\rangle_{R,L} = 0$. In comparison, for the non-Hermitian case ($\gamma \neq 0$ and u is complex), these relations are no longer satisfied, i.e., $|\nu\rangle_R \neq |\nu\rangle_L$ and ${}_{R,L}\langle -|+\rangle_{R,L} \neq 0$. However, given the definition of right/left eigenstates in Eq.20, the bi-orthogonality can be satisfied:

$${}_{L}\langle -|+\rangle_R = 0, \quad {}_{L}\langle +|-\rangle_R = 0. \quad (22)$$

Therefore, the normalization can be carried out between the right and left eigenvectors, namely, we require

$${}_{L}\langle \nu|\nu\rangle_R = 1, \quad \nu = \pm; \quad (23)$$

which gives

$$C_{\nu,L}^* C_{\nu,R} = \frac{1}{u + u^*}, \quad \nu = \pm. \quad (24)$$

Note that Eqs.(22,23) guarantees the commutation relation as Eq.4 in the main text. In this work, we choose a specific gauge such that the normalization factors are all real and identical:

$$C_{\nu,R} = C_{\nu,L} = \frac{1}{\sqrt{u + u^*}}. \quad (25)$$

In this way, when the \mathcal{PT} operator acts on these eigenvectors, we have

$$\begin{aligned} \mathcal{PT}|+\rangle_R &= u^*|+\rangle_R; & \mathcal{PT}|-\rangle_R &= -u^*|-\rangle_R; \\ \mathcal{PT}|-\rangle_L &= u^*|+\rangle_L; & \mathcal{PT}|-\rangle_L &= -u^*|-\rangle_L. \end{aligned} \quad (26)$$

These equations show that in the $\gamma < 1$ regime, $|\nu\rangle_{R/L}$ is the eigenvector of \mathcal{PT} operator with eigenvalue νu^* . If we choose a different gauge other than (25), the eigenvalues in (26) will be changed. However, the gauge choice will not affect the physical quantities studied in this work(such as the mean-field and LHY energies, Bogoliubov spectrum, etc), as long as (24) is satisfied.

II. Mean-field treatment

Given the commutation relation (Eq.4 in the main text) and the coherent ansatz (Eq.5 in the main text for the right state), we can obtain the following expectation values under the bi-orthogonal basis:

$$\begin{aligned} {}_L\langle \Psi_0 | \Psi_{\nu\mathbf{k}=0,R}^\dagger | \Psi_0 \rangle_R &= \sqrt{N_\nu} e^{-i\theta_\nu}, & {}_L\langle \Psi_0 | \Psi_{\nu\mathbf{k}=0,L} | \Psi_0 \rangle_R &= \sqrt{N_\nu} e^{i\theta_\nu}; \\ {}_L\langle \Psi_0 | \Psi_{\nu\mathbf{k}=0,R}^\dagger \Psi_{\nu'\mathbf{k}=0,L} | \Psi_0 \rangle_R &= \sqrt{N_\nu N_{\nu'}} e^{i(\theta_{\nu'} - \theta_\nu)}; \\ {}_L\langle \Psi_0 | \Psi_{\nu\mathbf{k}=0,R}^\dagger \Psi_{\nu'\mathbf{k}=0,R}^\dagger \Psi_{\nu''\mathbf{k}=0,L} \Psi_{\nu'''\mathbf{k}=0,L} | \Psi_0 \rangle_R &= \sqrt{N_\nu N_{\nu'} N_{\nu''} N_{\nu'''}} e^{i(\theta_{\nu'''} + \theta_{\nu''} - \theta_{\nu'} - \theta_\nu)}. \end{aligned} \quad (27)$$

This shows that in the mean-field framework under the bi-orthogonal basis, it is equivalent to replace the zero-momentum operators $\Psi_{\nu\mathbf{k}=0,R}^\dagger$ and $\Psi_{\nu\mathbf{k}=0,L}$ by their mean values, as shown by Eq.6 in the main text.

In re-writing the Hamiltonian as the form of Eq.7 in the main text, we can obtain the coupling constants in nine scattering channels as below:

$$\begin{aligned} U_{++;++} = U_{--;--} &= \frac{g}{V} \frac{u_-}{4}; & U_{++;--} = U_{--;++} &= \frac{g}{V} u'_+; & U_{+-;+-} &= \frac{g}{V} u_+; \\ U_{+-;++} = -U_{+-;--} &= U_{++;+-} = -U_{--;+-} = -\frac{g}{V} u'', \end{aligned} \quad (28)$$

with u_- , u_+ , u'_+ , u'' given in Eq.12 in the main text. The odd-parity couplings (in the second line of above equation) are purely imaginary, which is absent for the Hermitian case or with spin-independent interaction.

III. Bogoliubov analysis

We first derive the Heisenberg equation for non-Hermitian system under the bi-orthogonal basis. Given the definition of right and left states, at time t they evolve as

$$|\phi_R(t)\rangle = e^{-iHt}|\phi_R(0)\rangle, \quad (29)$$

$$|\phi_L(t)\rangle = e^{-iH^\dagger t}|\phi_L(0)\rangle, \quad (30)$$

here $|\phi_R(0)\rangle$ ($|\phi_L(0)\rangle$) is the initial right (left) state at $t = 0$. Define the time-dependent expectation value of operator \hat{A} as

$$\langle \hat{A} \rangle_t \equiv \langle \phi_L(t) | \hat{A} | \phi_R(t) \rangle, \quad (31)$$

we then have

$$\langle \hat{A} \rangle_t = \langle \phi_L(0) | e^{iHt} \hat{A} e^{-iHt} | \phi_R(0) \rangle, \quad (32)$$

and thus the Heisenberg equation can be written as

$$i \frac{\partial}{\partial t} \langle \hat{A} \rangle_t = \langle [\hat{A}, H] \rangle_t. \quad (33)$$

We can see that the form of Heisenberg equation (33) is identical to the Hermitian case. Nevertheless, it has a remarkable consequence for the non-Hermitian case, i.e., $\langle \hat{A}^\dagger \rangle_t \neq \langle \hat{A} \rangle_t^*$, which is very different from the Hermitian case. Similar relation for the time-dependent non-Hermitian operators has been given in Ref.[41].

Now we carry out the Bogoliubov analysis. The fluctuation Hamiltonian H_{BG} reads

$$H_{\text{BG}} = \sum'_{\mathbf{k}} \left\{ F_{\mathbf{k}}^T \mathcal{M}(\mathbf{k}) G_{\mathbf{k}} - \sum_{\nu} (\epsilon_{\nu\mathbf{k}} - \mu + gnu_{\nu}) \right\}, \quad (34)$$

where \sum' implies the summation be taken over half of \mathbf{k} -space to avoid the double counting; the vectors are

$$F_{\mathbf{k}} = \begin{pmatrix} \Psi_{-,\mathbf{k},R}^\dagger \\ \Psi_{-,-\mathbf{k},L}^\dagger \\ \Psi_{+,\mathbf{k},R}^\dagger \\ \Psi_{+,-\mathbf{k},L}^\dagger \end{pmatrix}, \quad G_{\mathbf{k}} = \begin{pmatrix} \Psi_{-,\mathbf{k},L} \\ \Psi_{-,-\mathbf{k},R}^\dagger \\ \Psi_{+,\mathbf{k},L} \\ \Psi_{+,-\mathbf{k},R}^\dagger \end{pmatrix}; \quad (35)$$

and the matrix \mathcal{M} read

$$\mathcal{M}(\mathbf{k}) = \begin{pmatrix} \epsilon_{-,\mathbf{k}} - \mu + gnu_- & 2gnu'_- e^{2i\theta_-} & 2gnu''_- & gnu'' e^{2i\theta_-} \\ 2gnu'_- e^{-2i\theta_-} & \epsilon_{-,\mathbf{k}} - \mu + gnu_- & gnu'' e^{-2i\theta_-} & 2gnu''_- \\ 2gnu''_- & gnu'' e^{2i\theta_-} & \epsilon_{+,\mathbf{k}} - \mu + gnu_+ & 2gnu'_+ e^{2i\theta_-} \\ gnu'' e^{-2i\theta_-} & 2gnu''_- & 2gnu'_+ e^{-2i\theta_-} & \epsilon_{+,\mathbf{k}} - \mu + gnu_+ \end{pmatrix}. \quad (36)$$

We aim to diagonalize H_{BG} as the following form:

$$H_{\text{BG}} = \sum'_{\mathbf{k}} \tilde{F}_{\mathbf{k}}^T \begin{pmatrix} E_{1\mathbf{k}} & & & \\ & E_{2\mathbf{k}} & & \\ & & E_{3\mathbf{k}} & \\ & & & E_{4\mathbf{k}} \end{pmatrix} \tilde{G}_{\mathbf{k}} + \text{const}, \quad (37)$$

where $E_{i\mathbf{k}}$ are the four eigen-modes for Bogoliubov quasi-particles, and the two eigen-vectors are

$$\tilde{F}_{\mathbf{k}} = \begin{pmatrix} \alpha_{1,\mathbf{k},R}^\dagger \\ \alpha_{2,\mathbf{k},L}^\dagger \\ \alpha_{3,\mathbf{k},R}^\dagger \\ \alpha_{4,\mathbf{k},L}^\dagger \end{pmatrix}, \quad \tilde{G}_{\mathbf{k}} = \begin{pmatrix} \alpha_{1,\mathbf{k},L} \\ \alpha_{2,\mathbf{k},R}^\dagger \\ \alpha_{3,\mathbf{k},L} \\ \alpha_{4,\mathbf{k},R}^\dagger \end{pmatrix}. \quad (38)$$

The eigen-operators are required to satisfy the commutation relation

$$[\alpha_{i,\mathbf{k},L}, \alpha_{j,\mathbf{k}',R}^\dagger] = \delta_{ij} \delta_{\mathbf{k}\mathbf{k}'}, \quad i, j = 1, 2, 3, 4. \quad (39)$$

To find out eigen-spectra $E_{i\mathbf{k}}$ as well as the relation between $\tilde{F}_{\mathbf{k}}, \tilde{G}_{\mathbf{k}}$ and $F_{\mathbf{k}}, G_{\mathbf{k}}$, we start from the EoMs of these vectors based on the Heisenberg equation (33). For the EoM of $G_{\mathbf{k}}$ and $\tilde{G}_{\mathbf{k}}$, we have

$$i \frac{\partial}{\partial t} G_{\mathbf{k}} = \begin{pmatrix} 1 & & & \\ & -1 & & \\ & & 1 & \\ & & & -1 \end{pmatrix} \mathcal{M}(\mathbf{k}) G_{\mathbf{k}}; \quad i \frac{\partial}{\partial t} \tilde{G}_{\mathbf{k}} = \begin{pmatrix} E_{1\mathbf{k}} & & & \\ & -E_{2\mathbf{k}} & & \\ & & E_{3\mathbf{k}} & \\ & & & -E_{4\mathbf{k}} \end{pmatrix} \tilde{G}_{\mathbf{k}}. \quad (40)$$

This implies that by diagonalizing the matrix $\text{Diag}(1, -1, 1, -1)\mathcal{M}(\mathbf{k})$, we can obtain the four Bogoliubov modes from its eigen-energies. Explicitly, by introducing a transformation matrix \mathcal{A} in $G_{\mathbf{k}} = \mathcal{A} \tilde{G}_{\mathbf{k}}$, we have

$$\mathcal{A}^{-1} \left[\begin{pmatrix} 1 & & & \\ & -1 & & \\ & & 1 & \\ & & & -1 \end{pmatrix} \mathcal{M}(\mathbf{k}) \right] \mathcal{A} = \begin{pmatrix} E_{1\mathbf{k}} & & & \\ & -E_{2\mathbf{k}} & & \\ & & E_{3\mathbf{k}} & \\ & & & -E_{4\mathbf{k}} \end{pmatrix}. \quad (41)$$

Similarly, we can write down the EoMs for $F_{\mathbf{k}}$ and $\tilde{F}_{\mathbf{k}}$, and by introducing a transformation matrix \mathcal{B} in $F_{\mathbf{k}}^T = \tilde{F}_{\mathbf{k}}^T \mathcal{B}$, we have

$$\mathcal{B} \left[\mathcal{M}(\mathbf{k}) \begin{pmatrix} -1 & & & \\ & 1 & & \\ & & -1 & \\ & & & 1 \end{pmatrix} \right] \mathcal{B}^{-1} = \begin{pmatrix} -E_{1\mathbf{k}} & & & \\ & E_{2\mathbf{k}} & & \\ & & -E_{3\mathbf{k}} & \\ & & & E_{4\mathbf{k}} \end{pmatrix} \quad (42)$$

Therefore, the Bogoliubov modes can also be obtained by diagonalizing the matrix $\mathcal{M}(\mathbf{k})\text{Diag}(-1, 1, -1, 1)$.

The two diagonalization schemes, i.e., one is based on (41) and the other is based on (42), produce the same solution of $E_{i\mathbf{k}}$, which satisfy

$$E_{\mathbf{k}} = \sqrt{\frac{-b_{\mathbf{k}} \pm \sqrt{b_{\mathbf{k}}^2 - 4c_{\mathbf{k}}}}{2}}, \quad (43)$$

with

$$\begin{aligned} b_{\mathbf{k}} &= -(\epsilon_{-;\mathbf{k}} - \mu + gnu_-)^2 - (\epsilon_{+;\mathbf{k}} - \mu + gnu_+)^2 - (gn)^2 (6u''^2 - 4u_+'^2 - 4u_-'^2); \\ c_{\mathbf{k}} &= [(\epsilon_{-;\mathbf{k}} - \mu + gnu_-)^2 - (2gnu_-')^2] [(\epsilon_{+;\mathbf{k}} - \mu + gnu_+)^2 - (2gnu_+')^2] + (gnu'')^2 [9(gnu'')^2 - 40(gn)^2 u_+ u_-'] \\ &\quad - 10(\epsilon_{-;\mathbf{k}} - \mu + gnu_-)(\epsilon_{+;\mathbf{k}} - \mu + gnu_+) + 16gnu_+'(\epsilon_{-;\mathbf{k}} - \mu + gnu_-) + 16gnu_-'(\epsilon_{+;\mathbf{k}} - \mu + gnu_+). \end{aligned} \quad (44)$$

The four eigen-modes in (43) fall into two identical pairs, and we choose $E_{1\mathbf{k}} = E_{2\mathbf{k}}$ and $E_{3\mathbf{k}} = E_{4\mathbf{k}}$. This is also a natural choice since in non-interacting limit, $\mathcal{M}(\mathbf{k})$ can exactly reduce to the diagonal matrix $\text{Diag}(E_{1\mathbf{k}}, E_{2\mathbf{k}}, E_{3\mathbf{k}}, E_{4\mathbf{k}})$ with $E_{1\mathbf{k}} = E_{2\mathbf{k}}$ and $E_{3\mathbf{k}} = E_{4\mathbf{k}}$.

In fact, based on Eq.(39) as well as Eq.4 in the main text, we can find the relation between the two transformation matrixes:

$$\mathcal{A} \begin{pmatrix} 1 & & & \\ & -1 & & \\ & & 1 & \\ & & & -1 \end{pmatrix} \mathcal{B} = \begin{pmatrix} 1 & & & \\ & -1 & & \\ & & 1 & \\ & & & -1 \end{pmatrix}, \quad (45)$$

and then one can prove straightforwardly that $\mathcal{B}\mathcal{M}(\mathbf{k})\mathcal{A} = \text{Diag}(E_{1\mathbf{k}}, E_{2\mathbf{k}}, E_{3\mathbf{k}}, E_{4\mathbf{k}})$. It follows that the first term in Eq.(34) is equal to the first term in Eq.(37). Therefore the constant terms in (34) and (37) are also equal. Further incorporating the regularization of bare couplings g and g_{12} from the mean-field interaction energy, we can obtain the Lee-Huang-Yang energy as Eq.14 in the main text.

In the following we present some analytical results for the property of excitation spectra :

(1). \mathcal{PT} -symmetry breaking in the regime $2\tilde{\Omega} < \eta < 1$ and with small γ : As discussed in the main text, in the regime $2\tilde{\Omega} < \eta < 1$ and $\gamma = 0$, all excitation spectra collapse to the single point at $k \equiv |\mathbf{k}| = k_0$ (Eq.15 in the main text). Then, as increasing γ from zero, the spectra will undergo \mathcal{PT} -symmetry breaking near $k \sim k_0$. The \mathcal{PT} -broken/unbroken boundaries in k -space are determined by the solutions to $b_{\mathbf{k}}^2 - 4c_{\mathbf{k}} = 0$ near $k \sim k_0$. In small γ limit, the solutions deviate from k_0 by a small shift $\delta \equiv |k - k_0|$, with:

$$\frac{\delta}{k_0} = \gamma \frac{(1-\eta)\sqrt{16\tilde{k}_0^4 + 2\tilde{k}_0^2(4 + 3\eta + 10\tilde{\Omega}) + (1+\eta)(2\tilde{\Omega} - \eta + 1)}}{4\tilde{k}_0^2(\eta - 2\tilde{\Omega})} + o(\gamma^2). \quad (46)$$

Here $\tilde{k}_0 = k_0/\sqrt{2mgn}$. The linear fit in Fig.2(c) in the main text is given by $k_1 = k_0 - \delta$ and $k_2 = k_0 + \delta$.

(2). Critical γ_c near $\eta \sim -1$: As discussed in the main text, γ_c is the critical value of γ when the lowest excitation energy turns from purely imaginary to purely real ($= 0$). This is determined by $c_{\mathbf{k}=0} = 0$, and thus

$$\frac{9\gamma_c^2(1-\eta)^2}{4} = -(1+\eta - 2\gamma_c^2) \left[2\tilde{\Omega}(1-\gamma_c^2)^{3/2} + (1-\eta)(1+\gamma_c^2) \right]. \quad (47)$$

We can see $\gamma_c = 0$ when $\eta = -1$, reproducing the mean-field collapse point for the Hermitian case. When η slightly deviate from -1 , we have

$$\gamma_c = \sqrt{-(1+\eta)\frac{2\tilde{\Omega}+2}{5-4\tilde{\Omega}}}, \quad (48)$$

which shows that γ_c scales as the square root of the deviation, as displayed by the orange dash-dot line in Fig.1 in the main text.

(3). Determination of γ_0 and γ_∞ : According to their definitions in the main text, γ_0 and γ_∞ , respectively, represent the value of γ when the excitation spectra at $k = 0$ and large $k \rightarrow \infty$ turn complex, i.e., $b_{\mathbf{k}}^2 - 4c_{\mathbf{k}} = 0$. It is then straightforward to find the value of γ_0 numerically, at which we have $b_{k=0}^2 = 4c_{k=0}$. To find out γ_∞ , we expand the function $F_{\mathbf{k}} \equiv b_{\mathbf{k}}^2 - 4c_{\mathbf{k}}$ at large $k \rightarrow \infty$, and only keep its leading order $\sim k^4$. γ_∞ is then determined by the coefficient of this leading term crossing zero, which gives the equation:

$$\eta^2 + \frac{4\gamma_\infty^2(\eta-1)}{1-\gamma_\infty^2} + 4\tilde{\Omega}^2(1-\gamma_\infty^2) = \frac{4\tilde{\Omega}(\eta+\gamma_\infty^2(\eta-2))}{\sqrt{1-\gamma_\infty^2}}. \quad (49)$$

We can see that the above equation support a solution $\gamma_\infty = 0$ at $\eta = 2\tilde{\Omega}$. This is also consistent with Eq.15 in the main text, which tells that the degenerate point k_0 goes to ∞ in the Hermitian case if $\eta = 2\tilde{\Omega}$.

IV. γ -induced droplet

The equilibrium density of the γ -induced droplet is determined by the zero-pressure condition: $E = \mu N$, or equivalently $\partial(E/N)/\partial n = 0$, with $E = E_{\text{mf}} + E_{\text{LHY}}$. By adopting Eqs.(9,17) in the main text, we obtain the equilibrium density n_{eq} as Eq.18 in the main text.

As reducing the particle number N , the kinetic term (quantum pressure) plays an important role and drives the droplet to gas transition. To estimate the critical number N_c at the transition, we take the similar strategy as in Ref.[27] and write down the extended Gross-Pitaevskii(GP) equation as

$$i\partial_t \Psi(\mathbf{r}) = \left(-\frac{1}{2m} \nabla_{\mathbf{r}}^2 + \frac{1-2\gamma^2+\eta}{2(1-\gamma^2)} g |\Psi|^2 + \frac{\partial \mathcal{E}_{\text{LHY}}}{\partial n} \right) \Psi(\mathbf{r}), \quad (50)$$

where $\Psi(\mathbf{r})$ is the wave function of the BEC and the particle number is determined by $N = \int d^3\mathbf{r} |\Psi(\mathbf{r})|^2$. By rescaling \mathbf{r} , Ψ , t through

$$\mathbf{r} = \tilde{\mathbf{r}}\xi, \quad \Psi = \tilde{\Psi}\sqrt{n_{\text{eq}}}, \quad t = \tilde{t}m\xi^2, \quad (51)$$

with

$$\xi = \sqrt{\frac{6(1 - \gamma^2)}{mgn_{\text{eq}}|1 - 2\gamma^2 + \eta|}}, \quad (52)$$

we can reduce the GP equation to

$$i\partial_t \tilde{\Psi}(\tilde{\mathbf{r}}) = \left(-\frac{1}{2}\nabla_{\tilde{\mathbf{r}}}^2 - 3|\tilde{\Psi}|^2 + \frac{5}{2}|\tilde{\Psi}|^3 \right) \tilde{\Psi}(\tilde{\mathbf{r}}). \quad (53)$$

It is found that Eq.53 share the same structure as the reduced GP equation in Hermitian case[27], which leads to the rescaled critical number $\tilde{N}_c \equiv \int d^3\tilde{\mathbf{r}}|\tilde{\Psi}|^2 = 18.65$ at the vanishing of droplet solution (droplet-gas transition). Given the scaling relation in (51), we can obtain the critical $N_c = n_{\text{eq}}\xi^3\tilde{N}_c$ as shown in the main text.
